Nitrogen nutrition impacts grapevine esca leaf symptom incidence, physiology and metabolism.

Ninon DELL'ACQUA[1], Gregory A. GAMBETTA[2], Gwenaëlle COMONT[1], Nathalie FERRER[1], Adam ROCHEPEAU[3,4], Pierre PÉTRIACQ[3,4], Chloé E. L. DELMAS[1,*]

[1]*INRAE, Bordeaux Sciences Agro, ISVV, SAVE, F-33140, Villenave d'Ornon, France*

[2]*EGFV, Bordeaux-Sciences Agro, INRAE, Université de Bordeaux, ISVV, 210 chemin de Leysotte, 33882 Villenave d'Ornon, France*

[3]*Univ. Bordeaux, INRAE, UMR1332 BFP, 33882 Villenave d'Ornon, France;*

[4]*Bordeaux Metabolome, MetaboHUB, PHENOME-EMPHASIS, 33140 Villenave d'Ornon, France.*

* *Correspondence: chloe.delmas@inrae.fr*

Number of figures: 8

Word count: 5 470

Number of Supplementary tables: 2

Number of Supplementary figures: 10

Running title: Nitrogen impact on plant physiology, metabolism and esca

ABSTRACT

Nitrogen plays a crucial role in plant growth and defence mechanisms, yet its role in plant-pathogen interactions is complex and remains largely unexplored, especially in perennial crops. This study aimed to investigate the effects of controlled nitrogen nutrition levels on disease incidence, fungal communities, and plant physiology and metabolism. Esca is a widespread grapevine vascular disease affecting physiology, xylem integrity and metabolism. Naturally infected *Vitis vinifera* L. cv. 'Sauvignon blanc' were subjected to three ammonium nitrate treatments across three seasons, resulting in reduced esca incidence under nitrogen deficiency compared with medium nutrition levels, while excess nitrogen had no significant impact. Nitrogen treatments significantly impacted vine physiology and leaf metabolites but did not affect fungal wood communities. Nitrogen deficiency significantly reduced stem diameter, photosynthesis, and leaf area, likely decreasing whole-plant transpiration, while excess nitrogen increased these factors suggesting a key role of plant transpiration in esca incidence. Additionally, nitrogen deficiency led to significantly higher production of phenylpropanoids, particularly antifungal flavonoids, in leaf metabolomes compared to the medium level. These findings highlight the pivotal role of nitrogen in the development of esca through alterations in vine morphology, physiology and metabolism. Fertilization practices may be crucial in the management of vascular diseases.

42 INTRODUCTION

43

44 Nitrogen is the most important nutrient that plants take up from the soil and, after water,
45 is the main limiting factor for plant growth (Vitousek and Howarth, 1991). Nitrogen plays a
46 crucial role in both the development and defence of plants, having a wide range of effects on
47 physiological and biochemical processes, and plant-pathogen interactions (Fagard *et al.*, 2014).
48 Plants can often experience nitrogen-stress conditions due to either nitrogen deficiency or
49 nitrogen excess from past and present fertilizer applications. Although viticulture is considered
50 as a crop with low fertilization demands compared to annual crops, nitrogen still plays an
51 important role in producing quality wine (Jackson and Lombard, 1993). Managing nitrogen in
52 vineyards is complex as it is an equilibrium between controlling vine vigor, maximizing grape
53 quality, mitigating environmental impact and managing fertilization costs (Verdenal *et al.*,
54 2021). At the plant level, managing nitrogen means finding the optimal balance between
55 growth (for optimal photosynthesis), defence capacity (against biotic and abiotic stresses), and
56 fruit quality.

57 Plant growth rate is one of the main traits influenced by nitrogen status. Nitrogen
58 deficiency induces a slowdown in vine growth resulting in a reduction in leaf area, a lower
59 number of leaves on secondary shoots, and faded green leaf color (Metay *et al.*, 2015; Vrignon-
60 Brenas *et al.*, 2019). Nitrogen deficit also changes the biomass allocation leading to biomass
61 reduction in annual organs in favour of perennial ones, such as trunks (Metay *et al.*, 2015).
62 Nitrogen excess, on the contrary, leads to a high vigour with a dense canopy and large dark
63 green leaves (Verdenal *et al.*, 2021).

64 Plant growth mostly relies on the production of primary metabolites, enzymes, and
65 structural proteins, which are synthesized from carbon assimilation during photosynthesis. The
66 functioning of the photosynthetic apparatus depends on nitrogen availability, as up to 75% of
67 the total nitrogen content of leaves is used in photosynthesis (Seepaul *et al.*, 2016) underpinned
68 by highly abundant enzymes like Rubisco and thylakoid proteins (Ferrario-Méry *et al.*, 1997).
69 Physiological responses involved in CO_2 assimilation such as stomatal conductance, net
70 photosynthesis, and transpiration could therefore be impacted by nitrogen levels (Zhang *et al.*,
71 2021). A correlation has been shown between nitrogen fertilization and CO_2 assimilation in
72 grapevines (Keller *et al.*, 2001; Schreiner *et al.*, 2013), except in Squeri *et al.* (2021). This
73 relationship may depend on plant age, localisation, nitrogen form or genotypes.

One assumption made in the literature is that, during moderate to strong nitrogen deficit, plant growth would be reduced to a greater extent than CO_2 assimilation leading to a carbohydrate over-accumulation (Herms and Mattson, 1992). This nitrogen-carbon imbalance would lead to a shift from primary metabolism to the production of secondary metabolites, including the accumulation of defence compounds which could impact immune response (Liao *et al.*, 2022). Integrated studies that combine plant health, growth, physiological, and metabolomic measurements could facilitate the evaluation of nitrogen's potential impact on defence metabolism (Massad *et al.*, 2012), and consequently, on the potential influence of nitrogen in plant-pathogen interaction.

Nitrogen levels influence plant resistance to disease (Huber and Watson, 1974), but depending on multiple factors such as concentration (Danial and Parlevliet, 1995), type of nitrogen fertiliser (Mur *et al.*, 2017), time of application (Abuley *et al.*, 2019), plant species (Mundy, 2008; Soulie *et al.*, 2020) and type of pathogens (Fagard *et al.*, 2014). The effect of tissue nitrogen concentration on plant susceptibility appears to depend on the pathogen species. In the case of tomato, there was no effect on susceptibility to *Fusarium oxysporum* (a hemibiotrophic pathogen), but susceptibility to *Pseudomonas syringae* (also hemibiotrophic) and *Oidium lycopersicum* (a biotrophic pathogen) increased significantly with nitrogen concentration (Hoffland *et al.*, 2000). However, a decrease in susceptibility to *Botrytis cinerea* (a necrotrophic pathogen) with increasing nitrogen concentration has been shown (Hoffland *et al.*, 1999). Finally, plants are likely to be more susceptible to biotrophic pathogens and more resistant to necrotrophic pathogens when fertilized with nitrogen (Dordas, 2008; Snoeijers *et al.*, 2000).

In grapevines, very little research has been done on nitrogen-plant-pathogen interactions. Most of the research has been done on *Botrytis cinerea*, *Erysiphe necator*, and *Plasmopara viticola* (Bavaresco and Eibach, 1987; Keller *et al.*, 2003; Mundy, 2008; Marcianò *et al.*, 2023), and demonstrated that pathogen severity increased with nitrogen supply. Studies have suggested that nitrogen may influence vascular disease by altering plant physiology, but no specific studies have been carried out so far (Destrac-Irvine *et al.*, 2007; Calzarano *et al.*, 2009). Among vascular diseases in vineyards, esca remains one of the most problematic because there is still no cure available. Esca is a complex disease associated with foliar symptoms, most commonly found in grapevines between 10 and 30 years old, depending on the cultivar (Etienne *et al.*, 2024; Gastou *et al.*, 2024). Foliar symptoms are observed randomly from one year to the next (Dewasme *et al.*, 2022) and are not reproducible by inoculating the fungal pathogens responsible for wood degradation and necrosis in the trunk (Mugnai *et al.*,

1999). The pathogenesis process of this vascular disease is still largely unexplained (Claverie *et al.*, 2020).

Nitrogen, which can influence water use efficiency, growth, and hydraulic traits, is likely to have a direct impact on esca pathogenesis. Recent works have highlighted the role of water transport within the plant and the influence of varietal water use efficiency on the development of esca leaf symptoms (Bortolami *et al.*, 2021*b*; Gastou *et al.*, 2024). A decrease in whole plant stomatal conductance and the reduction in CO_2 assimilation, stomatal conductance and WUE_i at symptomatic leaf level has been demonstrated in two grapevine varieties (Bortolami *et al.*, 2021*b*; Dell'Acqua *et al.*, 2023). An alteration in the radial stem growth during esca pathogenesis has also been recently reported (Bortolami *et al.*, 2021*b*; Dell'Acqua *et al.*, 2023). Esca is also known to impact grapevine leaf and fruit metabolomes (Lima *et al.*, 2017; Moret *et al.*, 2020; Ouadi *et al.*, 2021; Weiller *et al.*, 2024). Furthermore, esca is associated with different fungal pathogens and many of them are hemibiotrophic, i.e. organisms that live within living tissue for part of their lives and then continue to live in dead tissue (Bruez *et al.*, 2014, 2016, 2020; Elena *et al.*, 2018). On one hand, pathogen community composition could influence pathogen response to nitrogen fertilization. On the other hand, nitrogen fertilization could influence wood pathogen abundance, diversity and activity and thus esca pathogenesis.

This study aimed to investigate the effects of grapevine nitrogen nutrition on vascular pathogenesis while monitoring plant growth, physiology and metabolism, and trunk fungal communities. We hypothesized that under nitrogen deficit, the reduction in plant transpiration and the production of secondary metabolites would drive a decrease in leaf symptom incidence. Conversely, an excess of nitrogen could increase the incidence of esca leaf symptoms by enhancing plant growth and resource availability for pathogen development. We studied esca pathogenesis under different nitrogen conditions, using naturally infected mature *Vitis vinifera* cv. 'Sauvignon blanc' vines, transplanted from the field into pots and subjected to three different levels of nitrogen (in the form of ammonium nitrate) over three vegetative seasons.

MATERIALS AND METHODS

Plant material

The experiment was realized over three vegetative seasons (2021, 2022 and 2023) using 99 *Vitis vinifera* cv. 'Sauvignon blanc' vines, 81 grafted onto 101-14 Millardet et de Grasset (101-14 MGt) uprooted from INRAE Nouvelle-Aquitaine Bordeaux vineyard (44°47024.800N, 0°34035.100 W) in 2017, 2018 and 2019 and 18 grafted onto Fercal and uprooted from Couhins (44°45′17.9″N, 0°33′32.6″W) in 2020. The presence of esca leaf symptoms had been monitored in these vineyards at the plant level since 2012, following Lecomte *et al.* (2012). Plants were uprooted during late winter and transferred into 20L pots as described in Bortolami *et al.* (2019). Transplantation is the only method allowing the study of esca foliar symptom development under controlled conditions as it is only observed on mature plants in the field. Plants were pruned to retain four one-bud spurs on each of the two arms (and eight one bud spurs on one arm if there was only one remaining). The plants were installed in a polytunnel and distributed in six rows (two for each nitrogen level with an equivalent proportion of uprooting years and rootstocks). In 2021 and 2022, there were 32 plants in the lowest nitrogen level ($[NH_4NO_3]_{low}$), 33 plants in the middle level ($[NH_4NO_3]_{medium}$), and 34 plants in the highest nitrogen level ($[NH_4NO_3]_{high}$). During the 2022 season, two plants died : one in the low nitrogen level and the other in the medium level. Climate (i.e. humidity (in %) and temperature (in °C)) was monitored and from these parameters maximal vapor pressure deficit (*VPD*) was calculated for the three years experiments (Supplemental Fig. S1).

Fertilisation management

Three different nutritive solutions were prepared using varying concentrations of NH_4NO_3 (0.25 mM, 2 mM, and 8 mM for the $[NH_4NO_3]_{low}$, $[NH_4NO_3]_{medium}$, and $[NH_4NO_3]_{high}$ treatment, respectively) and, for all solutions, KH_2PO_4 (0.4 mM), $CaCl_2$ (0.75 mM), $MgSO_4$. $7H_2O$ (0.5 mM), K_2SO_4 (0.3 mM), and oligoelements. Plants were continuously drip-irrigated to ensure the absence of water stress (mean predawn water potential < -0.3MPa, data not shown). To maintain distinct plant nitrogen levels throughout the four-month period across the three nitrogen treatments, we conducted weekly monitoring of the plants using a N-tester. For each nitrogen level and date, three values (with 30 leaf measurements each) were obtained. If the plants from $[NH_4NO_3]_{low}$ exhibited a N-tester index that was too similar to $[NH_4NO_3]_{medium,}$ they were irrigated with the same nutritive solution as described above, but with $[NH_4NO_3]$ =

168 0 until the N-tester index differed. The same method was applied for $[NH_4NO_3]_{high}$ in
169 comparison to $[NH_4NO_3]_{medium}$. The mean N-tester index values over the season of
170 $[NH_4NO_3]_{low}$, $[NH_4NO_3]_{medium}$ and $[NH_4NO_3]_{high}$ (Supplemental Fig. S2) were aligned with
171 very low, medium and very high N-tester index identified in the literature (Van Leeuwen and
172 Friant, 2011). In addition, in the second and third years (ie. 2022 and 2023), we monitored
173 plants of the same cultivar ('Sauvignon Blanc') in an INRAE vineyard closeby the polytunnel
174 with no nitrogen nutrition problems (VITADAPT experimental block; (Destrac and van
175 Leeuwen) to manage the fertilization of the $[NH_4NO_3]_{medium}$ level according to the field N-
176 tester index (Supplemental Fig. S2) and the $[NH_4NO_3]_{low}$ and $[NH4NO3]_{high}$ as the first year.
177 To compare nitrogen level scores between the three treatments, we performed a linear mixed
178 model per year with the day of year set as a random effect and the nitrogen level treatment as
179 a fixed effect. A post-hoc Tukey test adjustment for multiple comparisons was realized. We
180 confirmed statistically that this method resulted in significantly higher and lower nitrogen
181 levels compared to medium level for each three years (P value < 0.001 for each treatment
182 comparison; Table S1). As we managed the $[NH4NO3]_{medium}$ level according to the vineyard,
183 we did not expect to have significantly the same values for the $[NH4NO3]_{medium}$ level and the
184 vineyard. However, in 2022 there was no significant difference in N-tester index between the
185 $[NH4NO3]_{medium}$ level and the vineyard (P value =0.056; Table S1).

186 *Esca leaf symptom notation*

187 Leaf symptom expression was monitored weekly over a four month-period at the leaf
188 and whole plant levels during all three years of the experiment. Esca leaf symptoms were
189 observed between July 19 and September 7, 2021, June 2 and September 7, 2022 and between
190 June 16 and August 22, 2023. During a season, phenotypes scored at whole plant level were
191 separated into 2 classes: symptomatic plants with symptomatic leaves and control plants with
192 no leaf symptom expression. The leaf level were separated into 3 classes: "C", leaf from control
193 plants, "S" symptomatic leaf from symptomatic plants and "AS", asymptomatic leaf from
194 symptomatic plants (both before and after symptom appearance), as done by Bortolami *et al.*
195 (2021*a*).

196 To compare leaf symptom expression between nitrogen levels, we performed a linear
197 mixed model with the year set as a random effect and the nitrogen level treatment as a fixed
198 effect. A post-hoc Tukey test adjustment for multiple comparisons was realized.

Vigor, stomatal density and gas exchange measurements

Plant growth measurements

Plant growth was assessed in control plants in each nitrogen level early September 2022 using (i) stem diameter at the third internode measured at 1 cm above the bottom node on the dorso-ventral axis, and (ii) the average length of three secondary shoots (taken from the sixth, seventh, and eighth nodes). These traits were measured in 20 control plants in $[NH_4NO_3]_{low}$,19 plants in $[NH_4NO_3]_{medium}$, and 18 plants in $[NH_4NO_3]_{high}$.

At the end of the season on November 30, 2023, the senescence stage was scored in control plants (n=86) and symptomatic plants (n=13) using the BBCH phenological scale (Lorenz *et al.*, 1995).

Leaf area

To estimate plant vigor, we calculated an average leaf area for each nitrogen level in control plants. On September 19, 2022, the area of approximately 100 healthy mature leaves from the middle of the canopy was measured using a LI-3000, LI-COR.

Stomatal density analysis

We used five leaves per nitrogen level to estimate stomatal density in control plants. As stomata are mainly located on the under leaf surface in grapevines, nail polish was applied under the leaf blade to the same location and left to dry for 30 minutes. The imprint was removed with transparent scotch tape. Three images were then taken for different localisations on each leaf impression, avoiding veins as much as possible, under a binocular magnifying glass with a Nikon SMZ1270 camera, and the NIS-ElementsD software associated with the magnifier. Each picture was analysed with imageJ by counting each stomata for the three localisations per leaf. The stomatal density was then assessed by dividing the number of stomata by the surface picture area in mm^2.

Leaf gas exchange

Ambient stomatal conductance (g_s) was measured with a Li-600 (LICOR) on control leaves between April 26 and September 9, 2022. Measurements were taken on control plants between 10h and 12h on 11 dates, on a total of 282 control leaves in the $[NH_4NO_3]_{low}$ level, 250 leaves in $[NH_4NO_3]_{medium}$, and 289 leaves in $[NH_4NO_3]_{high}$. To compare the ambient

228 stomatal conductance of symptomatic and control plants before symptom expression, we
229 retrospectively selected measurements of "AS" leaves (from plants that became symptomatic
230 later in the season) and "C" leaves (from control plants) taken in April and May 2022, on six
231 dates. We thus used measurements from 13 leaves in $[NH_4NO_3]_{low}$ level, 41 leaves in
232 $[NH_4NO_3]_{medium,}$ and 25 leaves in $[NH_4NO_3]_{high}$.

233 During symptom expression between July 6 and September 9, 2022 (5 dates), ambient
234 stomatal conductance of symptomatic leaves were measured in 8 "S" leaves from 2
235 symptomatic plants, 25 "S" leaves from 7 symptomatic plants and 19 "S" leaves from 4
236 symptomatic plants in $[NH_4NO_3]_{low}$, $[NH_4NO_3]_{medium,}$ and in $[NH_4NO_3]_{high}$ respectively.

237 Gas exchange was measured in the 2022 season between 9h and 12h on mature well-
238 exposed leaves from the middle of the stem of control asymptomatic plants using the
239 TARGAS-1 portable photosynthesis system (PP Systems). Cuvette Photosynthetic Active
240 Radiation was set to optimize photosynthesis (1500 µmol m^{-2} s^{-1}). The light-saturated
241 photosynthetic rate (*Amax* in µmol m^{-2} s^{-1}) and the maximum stomatal conductance (g_{smax} in
242 mmol m^{-2} s^{-1}) was recorded by alternating rows of plants (i.e. nitrogen levels). Measurements
243 were performed at four dates between July and September 2022 with a total of 35 leaves in the
244 $[NH_4NO_3]_{low}$ level, 56 leaves in $[NH_4NO_3]_{medium}$ and 38 leaves in $[NH_4NO_3]_{high}$.

245 The water use efficiency (WUE_i) was calculated as the ratio between light-saturated
246 photosynthetic rate (*Amax* in µmol m^{-2} s^{-1}) and maximum stomatal conductance (g_{smax} in mmol
247 m^{-2} s^{-1}).

248 **Statistical analyses**

249 To compare vigor (dorso-ventral stem diameter, lateral shoot length, and leaf area),
250 stomatal density, and gas exchange measurements (g_s, g_{smax}, A_{max} and WUE_i) of control
251 asymptomatic plants, between the three nitrogen levels, we performed ANOVAs, associated
252 with a post-hoc tukey test after normality was checked with a Levene test.

253 *Trunk fungal communities*

254 **Sampling method**

255 The trunk sampling was carried out in apparently healthy wood on September 21, 2022
256 using a drill at the level of the graft union. For each level of nitrogen fertilization, 10 control

257 vines were sampled and all the esca-symptomatic vines (n= 2, 7, and 4 plants in $[NH_4NO_3]_{low}$
258 , $[NH_4NO_3]_{medium}$ and $[NH_4NO_3]_{high}$, respectively) resulting in 43 wood samples. For each vine,
259 a 2cm^2 window in the bark was removed at the grafting point using a sterilized razor blade,
260 then cleaned with ethanol. If the wood was apparently healthy and free of necrotic lesions,
261 wood pieces were collected in a petri dish by drilling to a maximum depth of 1.5 cm using a
262 drill (Worx Power, Positec Germany) and a 0.7 mm drill bit cleaned between each vine. This
263 depth likely corresponds to functional wood in mature grapevines (McElrone *et al.*, 2021) and
264 is also the type of wood where a xylem discolored stripe developed during esca pathogenesis
265 (Lecomte *et al.*, 2024). We therefore hypothesize that this sampling site is a critical location
266 where pathogenic activity can occur. When necrotic wood was reached with the drill, a new
267 location was chosen as close as possible to the previous one. The wood pieces were placed in
268 2.5 mL tubes with a sterilized tweezer and directly immersed in liquid nitrogen. The samples
269 were then placed at -80°C until grinding by a tissue-lyser (TissueLyser II, Qiagen, Germany).

270 **DNA extraction**

271 For each sample, 60 mg was weighed and placed into a 2 ml µtube in liquid nitrogen.
272 Aliquots of 60 mg are stored at -80°C until extraction. We used the DNeasy Plant Mini Kit
273 (Qiagen) to extract the total genomic DNA according to the manufacturer's protocol. All
274 samples were diluted to obtain a maximum of 15 ng/µL of DNA. A negative extraction control
275 was included in the process.

276 **Fungal ITS1 amplification and Illumina MiSeq sequencing**

277 Two successive PCRs are used to amplify the targeted region and attach sample-
278 specific adapters and indexes on either side. The internal transcribed spacer 1 (ITS1) region of
279 the fungal ITS ribosomal DNA gene (Schoch *et al.*, 2012) was amplified with the ITS1F-ITS2
280 primers. Universal sequences were added to the specific sequences to enable hybridization of
281 adapters and sequencing indexes during 2nd PCR (i.e. mb-**ITS1F:** 5'-
282 TCGTCGGCAGCGTCAGATGTGTATAAGAGACAG**CTTGGTCATTTAGAGGAAGT**
283 **AA**-3' and mb-**ITS2:** 5'-
284 GTCTCGTGGGCTCGGAGATGTGTATAAGAGACAG**GCTGCGTTCTTCATCGATG**
285 **C**-3', with the specific sequences in bold).
286
287 The first PCR mixture (final volume = 25µl) consisted of 12.5µl of 2X mix PCR
288 platinum hot start (Invitrogen), 5.5µL eau DNase/RNase free, 2.5µl each of the forward and

289 reverse primers and 2µL of DNA template. PCR was performed using a thermocycler
290 (Mastercycler EP Gradient, Eppendorf, Germany) under the following conditions: initial
291 denaturation at 95°C for 2 minutes; followed by 35 cycles of 95°C for 45 s, 55°C for 60 s, and
292 72°C for 90 s; and a final extension phase at 72°C for 10 min. Two negative PCR controls were
293 included in the analysis. These PCR controls were subjected to the same amplification
294 procedure as all of the other samples used to rule out potential contaminants detected by
295 metabarcoding. The quality of the amplification products was checked by electrophoresis in
296 2% agarose in TBE 0.5X gels with 5µL of PCR product and 2µL of Zvision (2X) and migration
297 for 30min at 100V.
298 The second PCR and the amplicon sequencing (Illumina V3 kit: 2 × 300 bp paired-end
299 reads) were performed by the Genome Transcriptome Facility of Bordeaux according to
300 standard protocols.

301 **Bioinformatics and diversity analyses**

302 The bioinformatic analyses were carried out using the FROGS tools hosted by the
303 Galaxy platform (Escudié *et al.*, 2018). After obtaining the fastq sequences, the FROGS
304 preprocessing tool was used to associate R1 and R2 and obtain unique sequences. Then the
305 clustering, chimera removal, OTU (Operational Taxonomic Unit) filter, ITS sequence selection
306 and affiliation tools (blast on the database ITS UNITE Fungi 8.3), of the FROGS software were
307 used to obtain the abundance table. The data curation was made using the MetabaR package
308 (Zinger *et al.*, 2021) by taking into account the extraction and PCR controls (Table S2). When
309 necessary, OTUs were blasted on a database specific to grapevine trunk disease pathogens,
310 trunkdiseaseID.org. The MetabaR package was then used to transform the clean data obtained
311 to an object readable by the R phyloseq package v1.34.0 (McMurdie and Holmes, 2013).
312 In order to evaluate the impact of nitrogen level on the wood fungal communities,
313 control plants were used to calculate alpha and beta diversity indices. The observed, Shannon,
314 and Simpson alpha diversity indices of the trunk fungal communities were compared between
315 nitrogen levels using Kruskal Wallis tests. To visualize the dispersions among samples, we
316 performed ordination plots using a non-metric multidimensional scaling (NMDS) ordination
317 matrix based on Bray-curtis distance. Beta dispersion was calculated from transformed
318 centered log-ratio (CLR) data to test the overall differences in composition between nitrogen
319 level groups in control plants using a PERMANOVA. We were able to compare alpha and beta
320 diversity between control plants (n=10 for each nitrogen level) and symptomatic plants, only

321 in the medium and high nitrogen levels (n=4 and 7 symptomatic plants, respectively), as only
322 two plants were symptomatic in the low nitrogen level and thus excluded from the analysis.
323 To find associations between microbial features, nitrogen level, and symptoms, we
324 performed general linear models using MaAsLin2 (Mallick *et al.*, 2021). Fungal communities
325 analyses were performed using the phyloseq package in R (McMurdie and Holmes, 2013) and
326 MicrobiomeAnalyst 2.0 (Lu *et al.*, 2023).

327 *Untargeted metabolomic analysis*

328 **Sampling method**

329 The wood samples from control plants (n=30) used for metabarcoding were also used
330 for untargeted metabolomic analysis (10 mg of lyophilized wood samples).
331 Green leaves were sampled from randomly selected control plants (i.e. 17 plants in
332 $[NH_4NO_3]_{low}$, 13 plants in $[NH_4NO_3]_{medium}$ and 17 plants in $[NH_4NO_3]_{high}$) during the 2022
333 season in the different nitrogen nutrition levels and at different dates, always in the morning
334 (between 8h and 11h). They were selected on the primary shoots, at the same position and
335 exposure and directly placed in liquid nitrogen and then stored at -80°C until further analysis.
336

337 **Metabolomics of semi-polar extracts**

338 We extracted semi-polar compounds, including primary and secondary metabolites,
339 using automated high-throughput ethanol extraction procedures at the MetaboHUB-Bordeaux
340 Metabolome (https://metabolome.u-bordeaux.fr/) from 10 mg of freeze-dried grapevine leaves
341 and wood material, following previously established protocols (Luna *et al.*, 2020). Untargeted
342 metabolic profiling by UHPLC-LTQ-Orbitrap mass spectrometry (LCMS) was performed as
343 already reported (Dussarrat *et al.*, 2022; Martins *et al.*, 2022) using an Ultimate 3000 ultra-
344 high-pressure liquid chromatography (UHPLC) system coupled to an LTQ-Orbitrap Elite mass
345 spectrometer interfaced with an electrospray ionisation source (ESI, ThermoScientific,
346 Bremen, Germany) operating in negative ion modes as described previously (Luna *et al.*, 2020).

347 All 66 leaves (i.e. 20 leaves from $[NH4NO3]_{low}$, 22 leaves from $[NH_4NO_3]_{medium}$ and
348 24 leaves from $[NH_4NO_3]_{high}$) samples and 30 wood samples (i.e. 10 samples per nitrogen level
349 treatments) runs for the LCMS analytical sequence were randomised, extraction blanks
350 (prepared without plant material and used to rule out potential contaminants detected by

351 untargeted metabolomics), and Quality Control (QC) samples that were prepared by mixing 20
352 µL from each sample. QC samples were injected every 10 runs and used for i) the correction
353 of signal drift during the analytical batch, and ii) the calculation of coefficients of variation for
354 each metabolomic feature so only the most robust ones are retained for chemometrics
355 (Broadhurst *et al.*, 2018). Briefly, MS1 full scan acquisitions at high-resolution (240k) were
356 performed on QC samples and the various standards for exact mass measurements, and all
357 samples were subjected to MS2 Data Dependent Analysis (DDA, 30k resolution) to generate
358 fragmentation information for further annotation (Martins *et al.*, 2022).

359 **Processing of metabolomic data**

360 Raw LCMS data were processed using MS-DIAL v 4.9 (Tsugawa *et al.*, 2015). We also
361 implemented retention time correction in MS-DIAL, and the metabolomic signals were
362 normalised according to the LOWESS method based on the QC samples. We performed data-
363 curation according to blank check and setting thresholds as signal-to-noise ratio (SN) > 10,
364 coefficient of variation in quality controls < 30%. The 3184 final features for predictive
365 metabolomics annotations were performed using the MetaboHUB AgroMix in-house chemical
366 database and the FragHUB database (Dablanc *et al.*, 2024). Thus, putative annotation of
367 differentially expressed metabolites resulted from MS-DIAL screening of the MS1 detected
368 exact HR m/z and MS2 fragmentation patterns (Tsugawa *et al.*, 2015). Additionally, the
369 InChiKeys of annotated features were employed within ClassyFire to automatically generate a
370 structural ontology for chemical entities (Djoumbou Feunang *et al.*, 2016). Putative metabolites
371 that were unlikely to be found in leaves and woods (e.g. Human drugs) were considered as
372 misassigned and therefore reassigned as "Unknown".

373 **Statistical analysis**

374 Normalization to sample median, square root data transformation and Pareto scaling
375 were applied to metabolomic data. We performed principal component analysis (PCA) for leaf
376 and trunk samples to compare the metabolome of control plants between dates and between
377 nitrogen levels. Volcano plots were performed to identify biomarkers between treatments.
378 Thresholds were set at P value < 0.05 (Welch's t-test) and a twofold change threshold at FC >
379 1.5 using a Benjamini–Hochberg correction for false-discovery rate (FDR). Statistical analysis
380 was performed using Metaboanalyst and R.

381 RESULTS

382 *Nitrogen levels impacted esca incidence*

383 After three years of experiment, we found that plants under nitrogen deficiency
384 exhibited significantly fewer esca leaf symptoms than those with regular nitrogen nutrition (i.e.
385 6.4% ± 0.1 (± se) of symptomatic vines in $[NH_4NO_3]_{low}$ level vs. 19.5% ± 5.6 in
386 $[NH_4NO_3]_{medium}$ level; Fig. 1). The incidence of esca leaf symptoms under $[NH4NO3]_{high}$ was
387 13.7% ± 2.0 on average, and did not significantly differ from the two other levels (Fig. 1).

388 *Vine growth, leaf characteristics and senescence differed under different nitrogen levels in*
389 *control plants*

390 The vegetative growth of control plants was significantly impacted by nitrogen
391 nutrition. Stem diameter, secondary shoot length, and leaf area significantly increased with the
392 nitrogen level (*P* value < 0.05, ANOVA, Tukey post hoc, Fig. 2A,B,C). On the contrary, there
393 was no significant difference in stomatal density between the different nitrogen levels (Fig.
394 2D).
395 On November 30, 2023, 100% of the leaves of control vines had fallen in level
396 $[NH_4NO_3]_{low}$ (i.e.100% of control vines were stage 97 on the BBCH scale), 40% of the vines
397 had lost at least 50% of their leaves in $[NH_4NO_3]_{medium}$ level (i.e. 40% of control vines were at
398 least stage 95 on the BBCH scale) and none of the leaves had fallen in $[NH_4NO_3]_{high}$ level (i.e.
399 100% of control vines didn't have reached stage 93 on the BBCH scale) (Supplementary Fig.
400 S3). The same shift in senescence under low and high nitrogen level was observed in 2022 but
401 plant phenology was not monitored. We observed that when the symptomatic plants managed
402 to produce new green shoots, they exhibited delayed senescence compared to the control plants,
403 regardless of the nitrogen level treatment.

404 *Gas exchange in control plants differed under different nitrogen levels*

405 The ambient stomatal conductance measurements in control leaves evolved throughout
406 the 2022 vegetative season and significantly differed between nitrogen levels for several dates
407 during the season (*P* value < 0.05, ANOVAs, Supplemental Fig. S4). There was no difference
408 in ambient stomatal conductance between green leaves from control and future symptomatic
409 plants (data not shown). During symptom expression, ambient stomatal conductance of

410 symptomatic leaves was 23.8 ± 4.22 (se) mmol m^{-2} s^{-1} on average compared to 97 ± 3.8 (se)
411 mmol m^{-2} s^{-1} on average in control plants and did not vary significantly between nitrogen levels
412 (*P* value=0.3, ANOVA).

413 In control leaves, maximum CO_2 assimilation (A_{max}) was significantly lower under
414 $[NH_4NO_3]_{high}$ or $[NH_4NO_3]_{low}$ levels compared to $[NH_4NO_3]_{medium}$ level (*P* value < 0.05, Fig.
415 3A). The maximum stomatal conductance (gs_{max}) under $[NH_4NO_3]_{low}$ level did not significantly
416 differ from $[NH_4NO_3]_{medium}$ level. On the contrary, the gs_{max} was significantly reduced under
417 $[NH_4NO_3]_{high}$ level (*P* value < 0.05, Fig. 3B). Consequently, the water use efficiency at leaf
418 scale (*WUEi*) increased significantly with nitrogen levels (*P* value < 0.05, ANOVA, Tukey
419 post hoc, Fig. 3C).

420 **Trunk fungal communities in varying nitrogen levels and esca-symptomatic status**

421 After paired-end alignments and cleaning process 2,019,933 fungal ITS sequences were
422 generated from 41 samples, with an average of 49,266 fungal ITS sequences per sample (Table
423 S2). These reads have been assigned to 337 Operational Taxonomic Unit (OTU).

424 ***Fungal relative abundance***

425 In healthy wood samples, the 20 most abundant OTUs were identified as belonging to
426 the following genus: *Acremonium, Ambrosiella, Atrocalyx, Cladosporium, Devriesia,*
427 *Filobasidium, Fomitiporia, Neofusicoccum, Penicillium, Phaeoacremonium*, and
428 *Phaeomoniella.* In relative abundance, the proportions of these genus were found to vary
429 depending on the sample (Fig. 4).

430 The main fungal species associated with grapevine trunk diseases in the literature (i.e.
431 *Anthostoma decipiens, Botryosphaeria dothidea, Botryosphaeria stevensii, Cadophora luteo-*
432 *olivacea, Diaporthe ampelina, Diplodia seriata, Eutypa lata, Eutypa sp, Fomitiporia*
433 *mediterranea, Lasiodiplodia theobromae, Neofusicoccum parvum, Phaeoacremonium*
434 *minimum, Phaeomoniella chlamydospora, Phellinus punctatus, Pleurostoma richardsiae, and*
435 *Stereum hirsutum*) were found partly in almost all healthy wood samples from both control and
436 symptomatic plants (except for two control samples collected from the high nitrogen level)
437 (Supplemental Fig. S5).
438

439 ***Diversity indexes of fungal microbiota were not significantly affected by nitrogen level.***

Regarding alpha diversity (the diversity within samples), the fungal communities were not significantly different between nitrogen treatments in control plants from the 2022 season: observed diversity, Shannon (i.e. specific diversity) and Simpson (measuring the probability that two randomly selected individuals belong to the same species) indexes were not significantly different (P value > 0.05, Kruskal wallis tests, Fig. 5). Regarding beta diversity (i.e. the measurement of community dissimilarity), NMDS indicated no significant differences either between control plants (P value > 0.05, PERMANOVA, Supplemental Fig. S6). Using multiple linear regressions, we found that none of the species could be used as nitrogen level biomarkers.

Diversity indexes of fungal microbiota were partly affected by symptom expression.

When comparing the alpha diversity indexes of wood fungal microbiota from control and symptomatic plants, we found no significant differences in $[NH4NO3]_{medium}$ level, while the Shannon and Simpson indexes were significantly lower in symptomatic plants in $[NH4NO3]_{high}$ level (P value < 0.05, Wilcoxon test, Fig. 6A). In addition, we found a significant difference in beta diversity when comparing symptom-nitrogen level groups (P value < 0.05, PERMANOVA, Fig. 6B).

Using general linear models to search for associations between microbial features and symptomatology, pooling medium and high nitrogen levels, no microorganism specific to esca were identified. When searching for associations between microbial features and each nitrogen-esca treatment, we found that *Caloplaca sp.* significantly differentiated symptomatic plants in $[NH4NO3]_{medium}$ level from the other categories (control plants in $[NH4NO3]_{low}$, $[NH4NO3]_{medium}$ and $[NH4NO3]_{high}$ levels, and symptomatic plants in $[NH4NO3]_{high}$ level; P value < 0.05). In addition, *Verrucales sp.* were found to significantly differentiate symptomatic plants in $[NH4NO3]_{medium}$ level from control plants in $[NH4NO3]_{low}$ and $[NH4NO3]_{medium}$ nitrogen levels. However, no fungal biomarker was found to differentiate symptomatic plants of the $[NH4NO3]_{high}$ level from control plants from other treatments. None of the fungi associated with esca in the literature were identified as significant biomarkers to differentiate symptomatic plants from control ones.

Leaf and trunk metabolome variation between nitrogen levels, especially phenylpropanoid metabolites.

The leaf metabolism of control plants evolved over the course of the 2022 season (Supplemental Fig. S7). Consequently, we decided to separate the control samples in two time periods: early summer period, from June to the beginning of July 2022 and summer period, from the end of July to the beginning of August 2022. For both periods, PCA showed clear differences between the three nitrogen levels for control leaves (Fig. 7A,B). In order to study the metabolome associated with early symptom development, we focused on the early summer period.

Comparing the $[NH4NO3]_{low}$ level to the $[NH4NO3]_{medium}$ level of the early summer period, we found 47 metabolomic features significantly enriched in the low nitrogen level and 14 features significantly impaired (Fig. 8A). Putative metabolites annotated as primary metabolites, such as amino acids (e.g. glutamic acid), carbohydrates, and lipids (e.g. saccharolipids) were impaired in $[NH4NO3]_{low}$ level (Fig. 8B) while secondary metabolites, such as phenylpropanoids and benzenoids were enriched. The phenylpropanoids enriched in $[NH4NO3]_{low}$ were mainly flavonoids (Fig. 8C).

Comparing the $[NH4NO3]_{high}$ level to the $[NH4NO3]_{medium}$ level of the early summer period, we found 134 features significantly enriched in the high nitrogen level and 117 features significantly impaired (Fig. 8D). Among putative metabolites annotated, mainly amino acids, lignans, nucleosides, organic acids, organoheterocyclic compounds were enriched under $[NH4NO3]_{high}$ level, while terpenes, phenylpropanoids, benzenoids and carbohydrates were globally impaired (Fig. 8E). Among the phenylpropanoids, we observed an over-representation in flavonoids, isoflavonoids, and tannins under $[NH4NO3]_{high}$ level and an under-representation in diarylpropanoids, stilbenes, coumarines, and cinnamic acids (Fig. 8F).

Finally, comparing $[NH4NO3]_{low}$ level to $[NH4NO3]_{high}$ level in the early summer period, we found 390 features significantly enriched in the $[NH4NO3]_{high}$ level and 311 features significantly impaired (Fig. 8D). Mainly benzenoids and phenylpropanoids were enriched and organic and amino acids impaired in $[NH4NO3]_{low}$ level (Fig. 8H). The phenylpropanoids enrichment was driven by an over-representation in flavonoids (Fig. 8I).

According to the previously described results on the response of phenylpropanoids to nitrogen levels in the early summer period, we further explored their variability in the other period (summer). We found that the difference in phenylpropanoids between $[NH4NO3]_{low}$ level and $[NH4NO3]_{medium}$ level or $[NH4NO3]_{high}$ level was driven by an enrichment in

flavonoids also in the summer period (Supplemental Fig. 8B). In contrast to the early summer period, flavonoids were enriched in the $[NH4NO3]_{medium}$ level compared to $[NH4NO3]_{high}$ level (Supplemental Fig. 8D).

Regarding the trunk metabolome of control plants at the end of the season, PCA presented partial overlap between the three nitrogen levels (Fig. 7C). However, the discriminating volcano plot analysis showed 74 features enriched in $[NH4NO3]_{low}$ level compared to $[NH4NO3]_{medium}$ level and 77 impaired features (Supplemental Fig. 9A). Comparing the $[NH4NO3]_{high}$ level to the $[NH4NO3]_{medium}$ level, we found 124 features enriched and 117 features impaired (Supplemental Fig. 9C). In $[NH4NO3]_{low}$ level compared to $[NH4NO3]_{high}$ level, 196 features were enriched and 204 features were impaired (Supplemental Fig. 9E).

We found impaired levels of flavonoids and an enrichment in cinnamic acids in the $[NH4NO3]_{low}$ level compared to $[NH4NO3]_{medium}$ level. The differences between phenylpropanoids in the $[NH4NO3]_{medium}$ and $[NH4NO3]_{high}$ levels and between $[NH4NO3]_{low}$ and $[NH4NO3]_{high}$ levels were driven by the accumulation in flavonoid features in $[NH4NO3]_{medium}$ level and $[NH4NO3]_{low}$ level, respectively (Supplemental Fig. 9B,D).

Overall, metabolome analyses suggest a potential trade-off between primary and secondary metabolism depending on the level of stress (from deficit to excess) and the type of plant tissue (wood or leaf).

DISCUSSION

We investigated the effect of nitrogen deficiency or excess on the disease incidence, fungal wood communities, and plant physiology and metabolism during the vascular disease esca in *Vitis vinifera* cv. 'Sauvignon blanc' over a three-year experiment. We demonstrated that a deficit in nitrogen nutrition drastically reduced esca leaf symptom development, while an excess in nitrogen nutrition did not induce any significant difference compared to the medium nitrogen level. Through an integrative approach, we characterized plant physiological and biochemical changes with varying nitrogen fertilization, and demonstrated an absence of any impact on the wood fungal communities in control plants. This work provides new insights into the role of grapevine nutrition in the incidence of vascular disease and the putative underlying mechanisms.

536

537 *Impacts of nitrogen availability on plant growth*

538

539 Consistent differences in N-tester index over the years and increasing vigor with
540 increasing levels of nitrogen nutrition unequivocally confirmed the accuracy of the
541 experimental design. Furthermore, the senescence process was advanced under nitrogen deficit
542 and delayed under nitrogen excess, which is also well-documented in the literature (Agüera *et*
543 *al.*, 2010; Fan *et al.*, 2023).

544 *Impacts of nitrogen nutrition deficiency on esca incidence and plant physiology and*
545 *metabolism*

546

547 It is widely recognised that nitrogen availability has an influence on plant-pathogen
548 interactions (Fagard *et al.*, 2014). However, the nature of this impact remains complex and is
549 driven by multiple factors such as the host and pathogen species studied and the type of nitrogen
550 nutrition used. Here, we demonstrated that nitrogen deficiency led to a significant reduction in
551 esca incidence.

552 Under nitrogen deficiency conditions, plant vigor and the average leaf area were
553 reduced, as widely documented in the literature (Schreiner *et al.*, 2013). We can therefore
554 assume that nitrogen deficiency led to a reduction of the whole-plant (canopy) leaf area (as
555 shown in sorghum (Zhao *et al.*, 2005)). At the leaf level, we found no significant change in
556 stomatal density. CO_2 assimilation was reduced under nitrogen deficiency compared with
557 plants under medium nitrogen nutrition. This result was expected since more than half of the
558 nitrogen present in leaves is needed to synthesize the components of the photosynthetic
559 apparatus (Evans, 1989). Nitrogen deficiency could induce a reduction in the activity and
560 content of enzymes (such asRuBP and RuBISCO) and the concentration of chlorophyll (Dinu
561 *et al.*, 2022), which in turn negatively affects photosynthesis (Xie *et al.*, 2020). Schreiner *et al.*
562 (2013) also demonstrated that a reduction in nitrogen availability in Pinot Noir led to a decrease
563 in CO_2 assimilation. However, Squeri *et al.* (2021) who also worked on old potted vines (*Vitis*
564 *vinifera* cv. 'Barbera'), observed that photosynthesis was maintained under nitrogen deficit.
565 Furthermore, we found that a decrease in nitrogen availability did not impact stomatal
566 conductance when compared to the medium nitrogen level. Stomatal conductance has been
567 shown not to be regulated under nitrogen deficiency (Keller *et al.*, 1998). The reduced leaf area

568 and vigor, without any modification in stomatal density or stomatal conductance, likely led to
569 a reduction in transpiration at the whole-plant level.

570 It has been shown that reduced plant transpiration led to reduced esca leaf symptom
571 incidence (Bortolami *et al.*, 2021*b*), suggesting a key role of vine transpiration in esca
572 pathogenesis. In addition, plant vigor has been hypothesized to be positively correlated with
573 esca incidence in the vineyard but this hypothesis has rarely been tested. Only two recent
574 studies suggested that cultivars characterized by low vigor also exhibited low esca incidence
575 (Claverie *et al.*, 2024; Gastou *et al.*, 2024). Consequently, the reduced leaf symptom expression
576 under nitrogen deficit in our study may be triggered by the reduction of transpiring area
577 associated with the nitrogen deficiency treatment.

578 Nitrogen nutrition effects on plant disease expression may also be mediated by plant
579 metabolome modifications (Fagard *et al.*, 2014). The metabolome of control leaves varied
580 significantly with nitrogen nutrition throughout the summer season. By comparing nitrogen
581 deficiency with the medium nitrogen treatment in the early summer period, we showed a
582 decrease in carbohydrates, lipids and amino acids, and an increase in phenylpropanoids and
583 benzenoids. The decrease in primary metabolites in favor of secondary metabolites was
584 accentuated during the summer period (data not shown). In Fritz *et al.* (2006), during nitrogen
585 deficiency, the increase in phenylpropanoids was correlated with the induction of genes
586 involved in their metabolism, such as phenylalanine ammonia lyase (PAL). Rossouw *et al.*
587 (2017) also demonstrated that polyphenols and other products of the shikimate pathway were
588 affected by nitrogen availability. Therefore, these metabolomic analyses point to a profound
589 reorchestration of primary and secondary metabolisms in response to nitrogen levels, involving
590 some compounds already reported in previous nutritional studies of plant-pathogen
591 interactions. These results partly follow the carbon nutrient balance hypothesis (Bryant *et al.*,
592 1983) and the growth differentiation balance hypothesis (Herms and Mattson, 1992),
593 explaining that under limiting growth conditions, available resources would be more highly
594 allocated to defence production. However, this increase in defence metabolites is usually
595 associated with a maintenance of photosynthesis (Herms and Mattson, 1992). In our study, as
596 previously discussed, we found a reduction in CO_2 assimilation. However, in the case of
597 drought stress, some studies demonstrated an activation of secondary metabolism even though
598 photosynthesis was reduced (Ma *et al.*, 2014). We can assume that the remaining CO_2
599 assimilation was enough to support the production of secondary metabolites as the
600 photosynthesis demand was likely reduced due to reduced growth. Fluxomics analyses could
601 help address the flux imbalance between carbon and nitrogen pathways.

602 In our study, the increase in phenylpropanoids under nitrogen deficit was mainly due
603 to an accumulation of flavonoids at the leaf level. An increase in flavonoids under nitrogen
604 deficit has been described in numerous species (grapevine leaves (Squeri *et al.*, 2021); broccoli
605 leaves (Fortier *et al.*, 2010); and tomato leaves (Stewart *et al.*, 2001)). Flavonoids act as signals
606 in plant-microorganism interactions and are characterised by their anti-fungal and antioxidant
607 properties (Macheix *et al.*, 2005; Treutter, 2006). Studies have shown that a nitrogen-triggered
608 accumulation of soluble phenolic compounds can induce species-dependent resistance to
609 pathogens (Leser and Treutter, 2005). In our study, we are interested in nitrogen stress-induced
610 flavonoids, which can also be constitutively synthetised, but whose biosynthesis is enhanced
611 or inhibited by nitrogen stress. The anti-pathogenic properties of flavonoids may be non-
612 specific and result from their antioxidant properties. They could chemically process excess
613 ROS generated by the plant during infection, but this is still a matter of debate (Hernández *et*
614 *al.*, 2009; Decros *et al.*, 2019). Flavonoids are also involved in the hypersensitivity response,
615 which is the primary defence mechanism of infected plants, and in programmed cell death
616 (Treutter, 2006). An increase in these flavonoids during nitrogen deficiency could therefore
617 prevent the development of symptoms by stimulating plant defences.
618 Similarly to leaves, nitrogen deficiency enhances plant defence secondary metabolites
619 in wood. However, it was not triggered by flavonoids as shown in leaves. As the wood was
620 sampled late in the season compared to leaf sampling, further research during the same period,
621 earlier in the summer, should be conducted to get a better view of this secondary metabolism
622 induction under nitrogen deficiency.
623
624 *Impact of excess nitrogen nutrition on esca incidence and plant physiology*
625
626 In contrast to nitrogen deficiency, excess nitrogen had no significant impact on esca
627 leaf symptom development compared to the medium nitrogen treatment. Many studies only
628 included two different nitrogen levels (Keller *et al.*, 2003; Squeri *et al.*, 2021). However, it has
629 been shown that physiological responses are not necessarily linear with nitrogen nutrition
630 (Bondada and Syvertsen, 2003; Zheng *et al.*, 2022). Excess nitrogen also had an impact on
631 physiology compared with average nitrogen, but through a different process to that of nitrogen
632 deficiency. Under nitrogen excess, the vigor of the plant increased, as well as the leaf surface
633 area, without any change in stomatal density. The transpiring surface area was therefore
634 increased, which might be expected to result in an increase in leaf symptoms compared to
635 medium nitrogen level. However, this increase was compensated at leaf level by lower stomatal

636 conductance, leading to a reduction in CO_2 uptake. This regulation enabled plants to increase
637 their *WUEi.* We can therefore assume that the whole plant stomatal conductance was likely
638 maintained, with consequently no significant differences with medium nitrogen level in terms
639 of plant transpiration and leaf symptom incidence.

640 These physiological modifications are likely associated with altered plant metabolism.
641 As such, we demonstrated a modification of the metabolome from high nitrogen level plants
642 compared to medium nitrogen level. However at leaf scale, these modifications changed across
643 the season. In early summer, phenylpropanoids were more abundant in control leaves and
644 healthy wood from medium nitrogen levels than in those from high nitrogen levels, as opposed
645 to mid-summer when the converse was true. This variable response was consistent with the
646 absence of a significant difference in the incidence of esca symptoms between these two
647 nitrogen levels.

648 *Nitrogen nutrition did not significantly modified the wood fungal communities in control plants*

649 The main research studies assessing the impact of nitrogen fertilization on fungal
650 communities have focused on soil communities (Ullah *et al.*, 2019) and, more rarely, on
651 leaf/shoot communities (Borruso *et al.*, 2021). In our case, since the pathogens associated with
652 esca are usually detected only in the trunk, we focused on the trunk fungal communities. We
653 identified fungal taxa potentially associated with esca and other grapevine trunk diseases in the
654 literature in all healthy (i.e. non necrotic) wood samples from symptomatic plants and control
655 plants (except in two samples from the high nitrogen level). Our results showed that the wood
656 fungal communities of control plants were not affected by nitrogen nutrition at the end of 2022
657 the season. We can hypothesize that either two seasons of differential nutrition was too short
658 to modify the diversity and composition of the fungal communities, or that the trunk microbiota
659 is relatively stable. Trunk microbiota has been shown to vary during the season (Bruez *et al.*,
660 2014, 2020), but we can assume this would not therefore be due to variation in nitrogen
661 availability. This is consistent with the fact that, in contrast to the large differences obtained in
662 leaf metabolism between nitrogen levels during the growing season, differences in the
663 metabolome of healthy wood were much less pronounced (illustrated via the PCA analysis).

664 In addition, we found that fungal pathogen inoculations (*Neofusicoccum parvum* and
665 *Phaeomoniella chlamydospora*) on wood cuttings collected from the three nitrogen levels did
666 not show any differences of necrotic lesion length (supplemental Method 1 and Fig S10). This

667 additional result suggests that nitrogen fertilization has no impact on Sauvignon blanc
668 susceptibility to these two trunk pathogens or conversely on the fungal strains' pathogenicity.

669 *Fungal communities in healthy wood partly differ between symptomatic plants and control*
670 *plants*

671 A significant difference in alpha diversity between symptomatic plants and control
672 plants was only shown in the high nitrogen level. In addition, no pathogens associated with
673 esca in the literature could be identified as biomarkers between control and symptomatic
674 samples regardless of the nitrogen level. However we demonstrated that symptomatic plants
675 from the medium (field-like) nitrogen level could be distinguished from other treatments by
676 two ascomycota, one *Verrucariales sp* and one *Caloplaca sp.* The latter has already been
677 identified in esca-symptomatic plants (Del Frari *et al.*, 2019). We can conclude that even if we
678 demonstrated some differences, the global fungal communities in healthy wood did not differ
679 strongly between nitrogen levels and presence/absence of esca leaf symptoms. We might
680 assume that nitrogen fertilization could impact pathogen activity and aggressiveness, although
681 we were unable to demonstrate this through the inoculation of two pathogens in woody cuttings
682 collected from the three different nitrogen levels. However, the wood sampling was realised
683 after the onset of symptom expression. Further research should investigate the impacts of
684 nitrogen level and symptom formation on fungal communities across the whole vegetative
685 season, especially prior to symptom formation and at the symptom onset. This would allow the
686 identification of any possible shift in communities that could explain the development of
687 symptoms and/or a possible imbalance within the communities depending on nitrogen level.

688 CONCLUSION

689 To conclude, our three-year investigation into the effects of nitrogen fertilization on
690 esca pathogenesis in 'Sauvignon blanc' demonstrated a significant impact on leaf symptom
691 expression. Our integrative approach revealed physiological and biochemical changes induced
692 by nitrogen nutrition, likely underlying the observed esca variability. This study highlights that
693 nitrogen nutrition could be a lever in managing the expression of foliar symptoms of vascular
694 diseases. Exploring the effects of different nitrogen nutrition methods in a range of cultivars
695 and wine regions may provide new insights into the understanding of esca leaf symptom
696 expression in the vineyard.

Acknowledgements

We thank the experimental teams of UMR SAVE (INRAE, Bordeaux, France) for providing the materials, logistics, and assistance during the experiment. In particular we are very thankful to Marie Chambard and Mathéo Pinol Daubisse for assistance in gas exchange measurements and wood sampling. We thank Jérôme Jolivet, Sebastien Gambier (UMR SAVE) and Jean-Pierre Petit (UMR EGFV) for providing technical knowledge and support for plant transplantation and maintenance. We are grateful to Cédric Cassan (UMR BFP) for the extraction and LCMS analysis, and to Adam Rochepeau (UMR BFP) for the MS-DIAL analysis. Part of the experiments (ITS sequencing) were performed at the Genome Transcriptome Facility of Bordeaux (Grants from Investissements d'avenir, Convention attributive d'aide EquipEx Xyloforest ANR-10-EQPX-16-01).

This work was supported by the project ESCAPADE (22001436) (program "Plan National Dépérissement du Vignoble", FranceAgriMer/CNIV), the Nouvelle-Aquitaine region (project VITIPIN, 22001439), and received financial support from the French government in the framework of the IdEX Bordeaux University "Investments for the Future" program / GPR Bordeaux Plant Sciences, and from MetaboHUB (ANR-11-INBS-0010).

Author contributions

N.D.A., C.E.L.D., G.A.G., designed the experiments;

N.D.A., C.E.L.D., and N.F. conducted the esca symptom notations, nitrogen fertilization management, and wood sampling;

N.D.A. and N.F. carried out the leaf samplings, measured vigor, leaf gas exchange and area;

P.P. and the MetaboHUB-Bordeaux team carried out of untargeted metabolomic measurements (extraction and MS-DIAL analysis);

G.C. realized the experiment of controlled inoculations of wood pathogens and analyzed the associated dataset presented in supplementary material;

N.D.A. wrote the first draft of the article under the supervision of C.E.L.D. and G.A.G.;

all authors participated in scientific discussion regarding the experiments and methodologies used, edited, and agreed on the last version of the article.

Data availability

Ecophysiological and morphological trait measurements, leaf and trunk metabolome datasets, raw and processed ITS sequence data and associated metadata used for this article will be achieved in a public repository (data.gouv.fr) after acceptance of the publication.

729 FIGURES

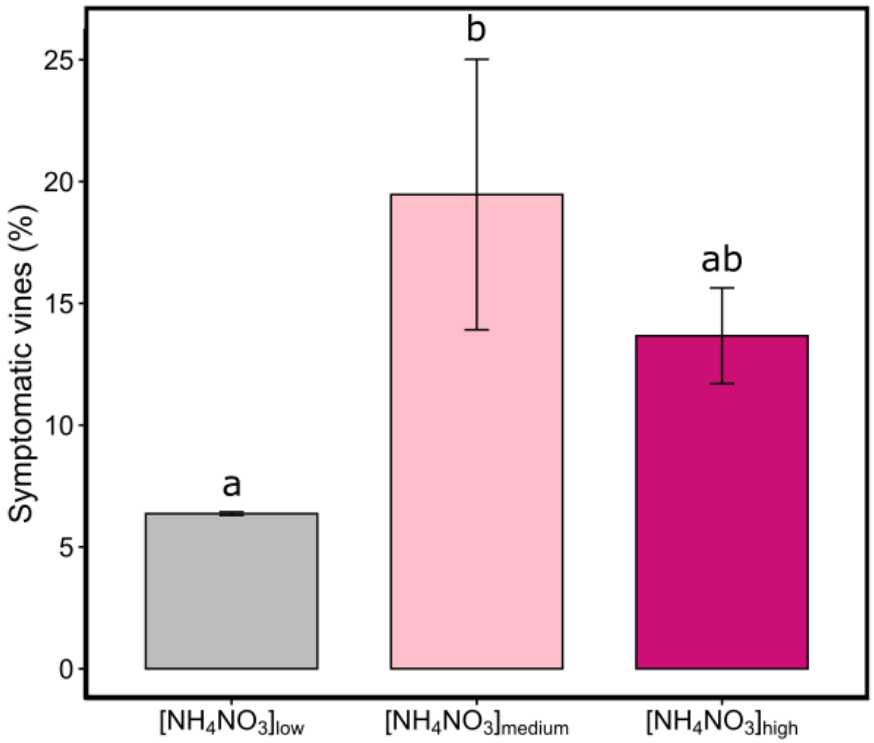

730

731 **Figure 1. Mean percentage of esca-symptomatic vines (*Vitis vinifera* cv. 'Sauvignon blanc')**
732 **according to the three levels of nitrogen nutrition during the three experiment seasons.**
733 Low nitrogen level ($[NH4NO3]_{low}$) is represented in grey, medium nitrogen level
734 ($[NH4NO3]_{medium}$) in pink and high nitrogen level ($[NH4NO3]_{high}$) in dark pink. Error bars are
735 standard errors. To compare leaf symptom expression between nitrogen levels, we performed
736 a linear mixed-effects model with the year set as a random effect and the nitrogen level
737 treatment as a fixed effect. Letters represent significant differences (P value < 0.05, n = 31-34).
738 The horizontal line in the box represents the median value.
739

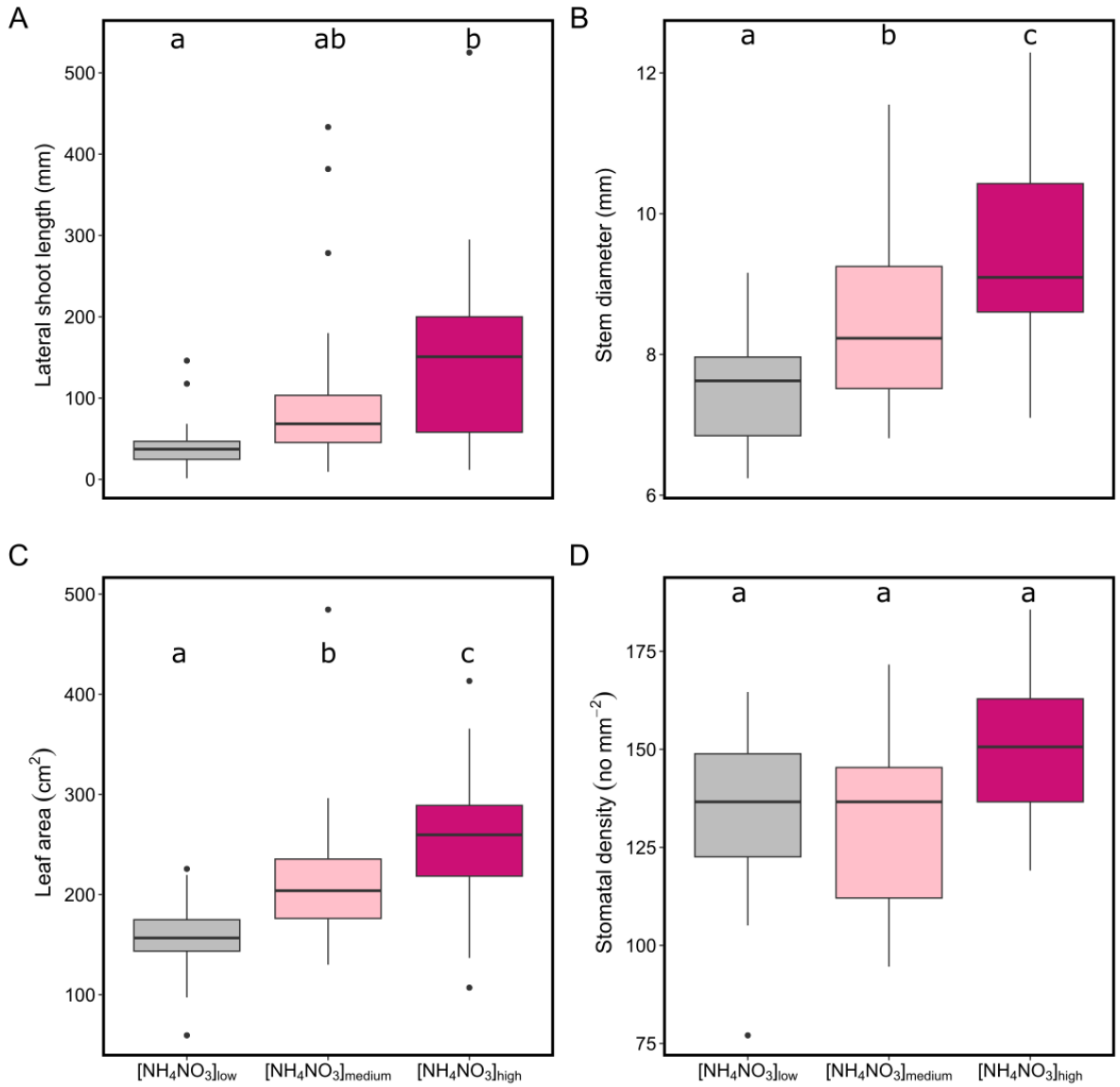

Figure 2. Growth and structural traits of *Vitis vinifera* cv. 'Sauvignon blanc' plants subjected to three different nitrogen nutrition levels in 2022. (A) Lateral shoot length (in mm) and (B) dorso-ventral stem diameter (in mm) were measured on 20 plants in $[NH_4NO_3]_{low}$, 19 plants in $[NH_4NO_3]_{medium}$, and 18 plants in $[NH_4NO_3]_{high}$, (C) leaf area of ~100 leaves from each nitrogen level (in cm^2), (D) leaf abaxial stomatal density (5 leaves per nitrogen level, in no mm^{-2}). The horizontal line in the box represents the median value. The letters indicate significant differences in ANOVAs (P value < 0.05, post-hoc tukey test). The horizontal line in the box represents the median value.

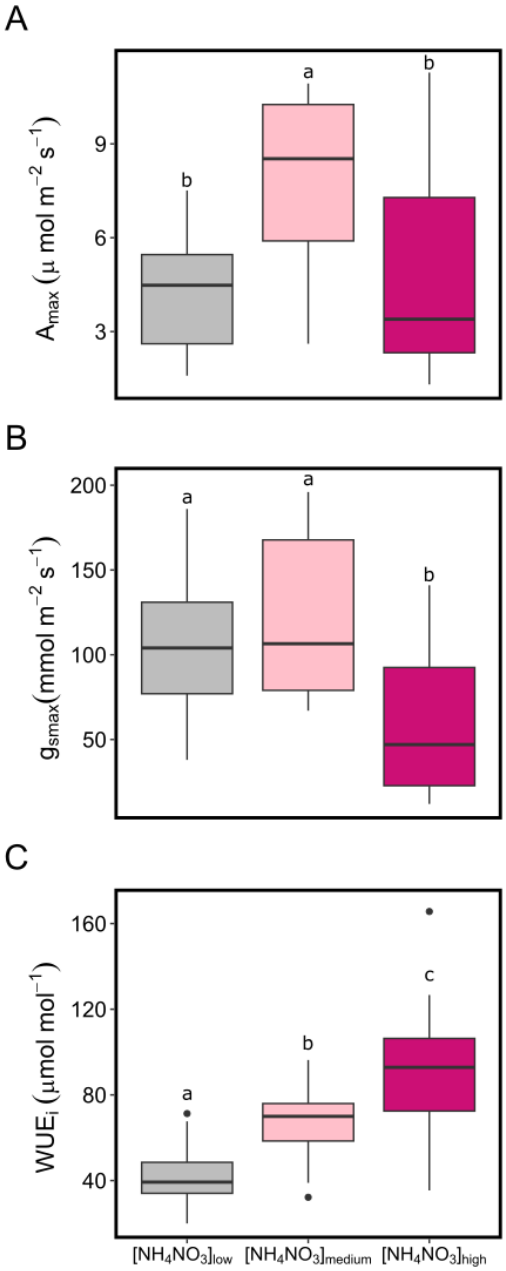

Figure 3. Leaf physiological traits of *Vitis vinifera* cv. 'Sauvignon blanc' plants subjected to three different nitrogen nutrition levels during the 2022 season. (A) light-saturated photosynthetic rate (A_{max} in µmol m^{-2} s^{-1}), (B) maximum stomatal conductance (gs_{max}, in mmol m^{-2} s^{-1}), (C) water use efficiency (WUE_i, in µmol m^{-2} s^{-1}). The measurements were made on 35 control leaves in [NH$_4$NO$_3$]$_{low}$, 56 leaves in [NH$_4$NO$_3$]$_{medium}$, and 38 leaves in [NH$_4$NO$_3$]$_{high}$. The letters indicate significant differences in ANOVAs (P value < 0.05, post-hoc tukey test). The horizontal line in the box represents the median value.

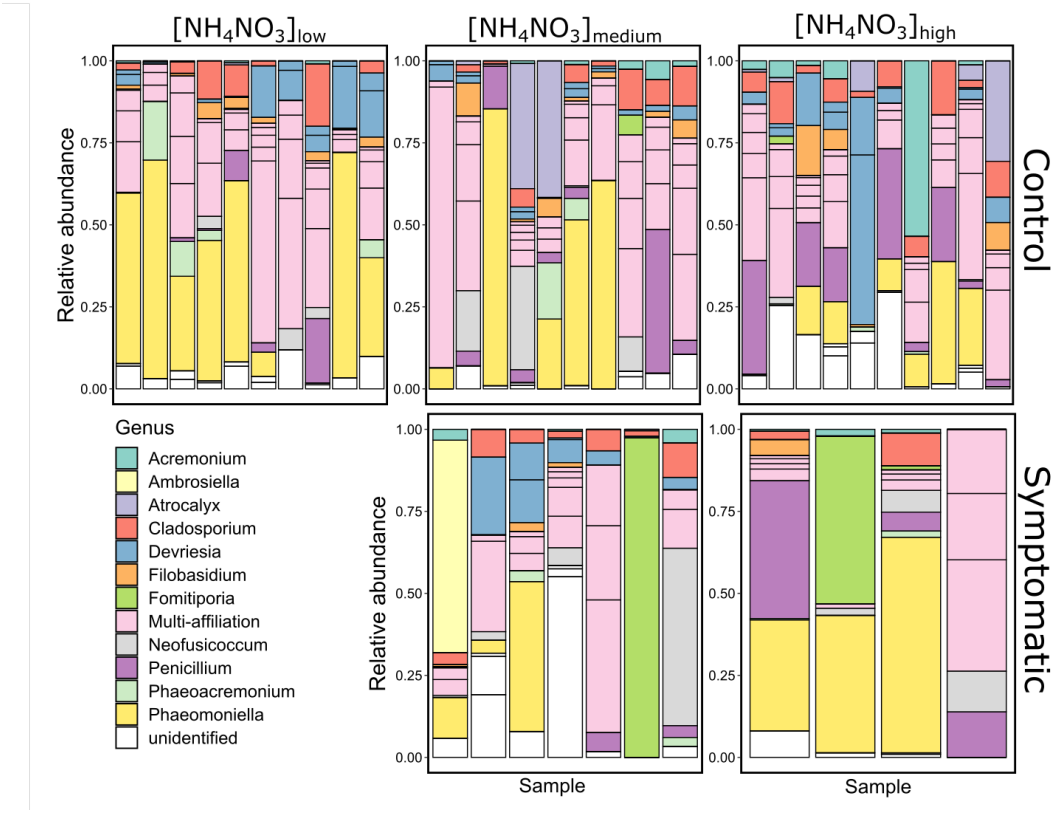

Figure 4. Relative abundance of the top 20 fungal Operational Taxonomic Unit (OTU) classified by genus in control and symptomatic *Vitis vinifera* cv. 'Sauvignon blanc' trunk samples (healthy wood) from the three nitrogen levels. Each bar represents one sample. Note the absence of samples from symptomatic plants in the $[NH_4NO_3]_{low}$ level, as only two plants were symptomatic (not sampled).

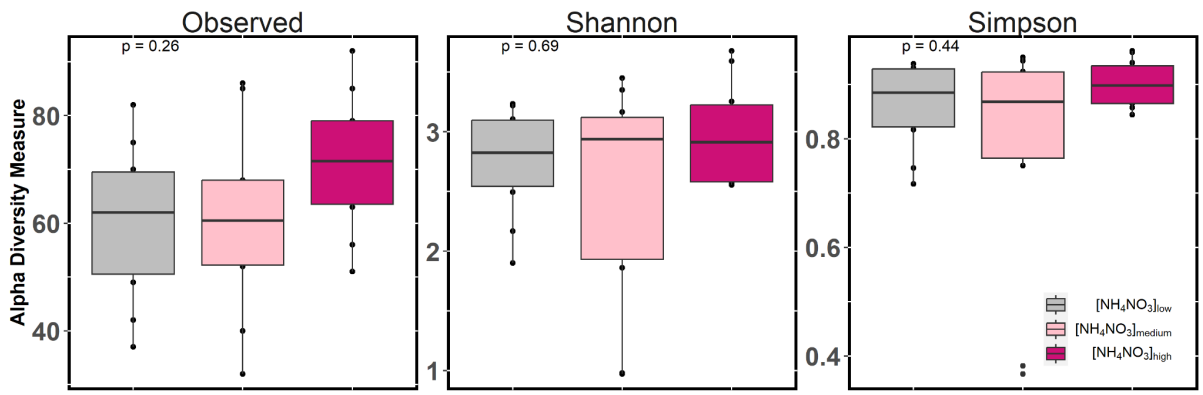

Figure 5. Observed, Shannon, and Simpson alpha diversity indices of the trunk fungal communities in healthy wood of control plants under three nitrogen levels. No significant differences were found between treatments (*P* value > 0.05, Kruskal Wallis test). The horizontal line in the box represents the median value.

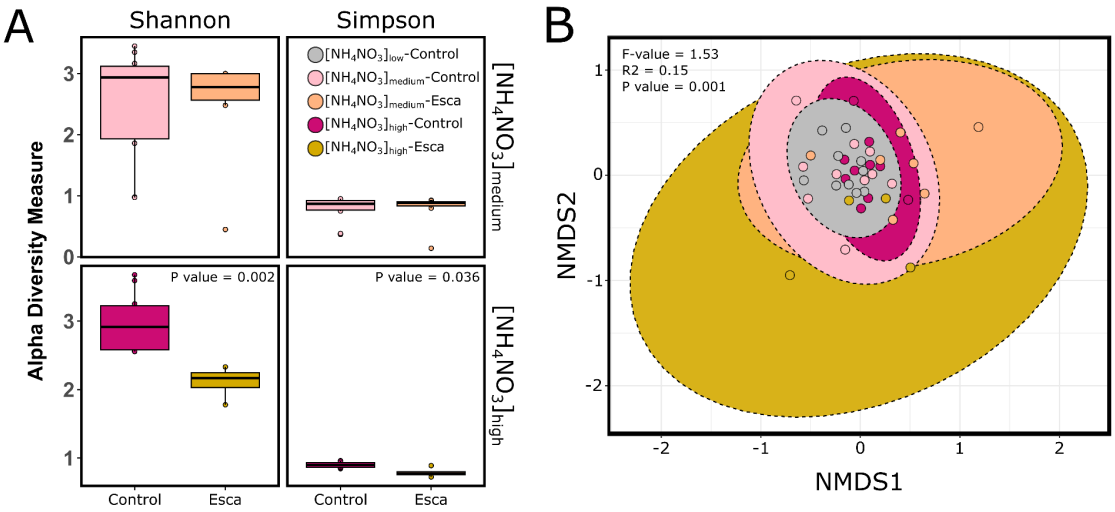

Figure 6. Analysis of fungal communities from healthy wood between control and symptomatic *Vitis vinifera* cv. 'Sauvignon blanc' and nitrogen level treatments. (A) Shannon and Simpson alpha diversity indices, (B) Beta diversity. Five groups were compared in the analysis: $[NH_4NO_3]_{low}$ - Control (n=10, in grey), $[NH_4NO_3]_{medium}$ - Control (n=10, in pink) , $[NH_4NO_3]_{medium}$ - Esca (n=7, in orange), $[NH_4NO_3]_{high}$ - Control (n=10, in dark pink) and $[NH_4NO_3]_{high}$ - Esca (n=4, in yellow). Significant differences have been found between treatments in alpha diversity measurements (only *P* value < 0.05 are indicated in the figure, Kruskal Wallis test). The horizontal line in each box plot (A) represents the median value. Beta dispersion was calculated from transformed centred log-ratio (CLR) data to test the difference in dissimilarity between nitrogen level groups using a PERMANOVA (F value = 1.53, R^2 = 0.15, *P* value = 0.001).

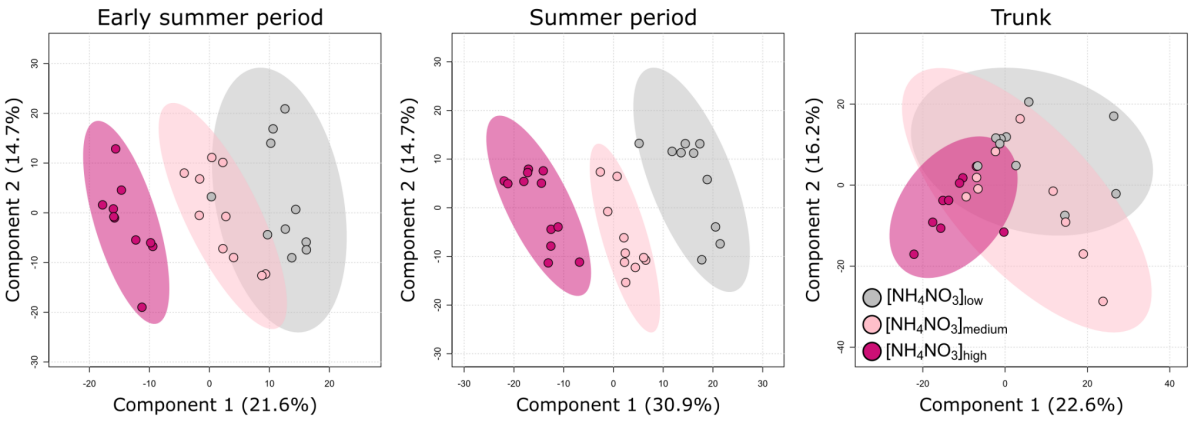

Figure 7. Principal component analysis (PCA) of metabolic profiles in leaves and trunks of *Vitis vinifera* cv. 'Sauvignon blanc'. PCAs compare the three nitrogen levels in control leaves collected during (A) the early summer period (June 7, 2022 June 24, 2022 and July 4, 2022) and (B) the summer period (July 21, 2022, August 10, 2022), and (C) trunk samples collected on September 12, 2022. Colored circles arbitrarily enclose treatment types: low nitrogen level $[NH_4NO_3]_{low}$ (in grey), medium nitrogen level $[NH_4NO_3]_{medium}$ (in pink), and high nitrogen level $[NH_4NO_3]_{high}$ (in dark pink).

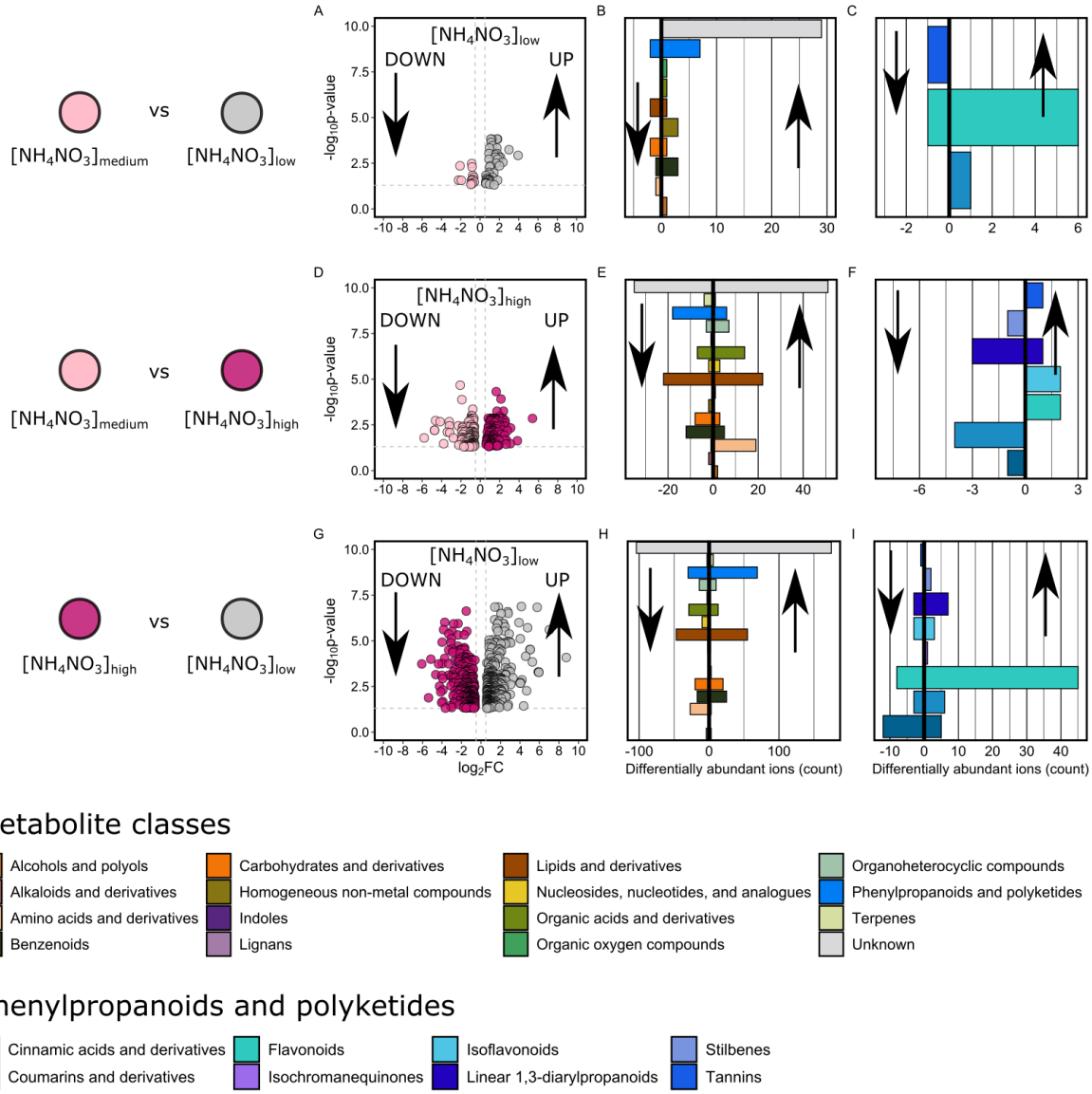

Figure 8. Quantitative differences in metabolite abundance between nitrogen levels in leaves from the early summer period (i.e. june-july) (*Vitis vinifera* cv. 'Sauvignon blanc'). First line represents the comparison analysis between $[NH_4NO_3]_{low}$ and $[NH_4NO_3]_{medium}$ (A,B,C), second line represents the comparison between $[NH_4NO_3]_{medium}$ and $[NH_4NO_3]_{high}$ (D,E,F), and the third line represents the comparison analysis between $[NH_4NO_3]_{high}$ and $[NH_4NO_3]_{low}$ (G,H,I). (A,D,G) Volcano plots expressing statistical enrichment ("UP") and impairment ("DOWN") of features (Welch's t-test) as a function of fold difference in each differential treatment comparison. Data shown represent negative (Electrospray ionization, ESI–) features from extractions. Cut-off values were set at P value < 0.05 and fold change > 1.5), using a Benjamini–Hochberg correction for false-discovery rate (FDR). (B,E,H) Class assignment of the putative metabolites selected through the volcano plots, either enriched ("UP" arrows) or impaired ("DOWN" arrows). Class assignment was performed using

Classyfire and literature. Multiple features putatively annotating to the same metabolite were counted additively in the metabolite classes. Putative metabolites that are unlikely to accumulate as natural products (e.g. drugs) were classified as unknown along with feature markers that could not be assigned to any known compound. (C,F,I) Overview the phenylpropanoids and polyketides class.

REFERENCES

Abuley IK, Nielsen BJ, Hansen HH. 2019. The influence of timing the application of nitrogen fertilizer on early blight (*Alternaria solani*). Pest management science **75**, 1150–1158.

Agüera E, Cabello P, de la Haba P. 2010. Induction of leaf senescence by low nitrogen nutrition in sunflower (*Helianthus annuus*) plants. Physiologia plantarum **138**, 256–267.

Bavaresco L, Eibach R. 1987. Investigations on the influence of N fertilizer on resistance to powdery mildew (*Oidium tuckeri*) downy mildew (*Plasmopara viticola*) and on phytoalexin synthesis in different grapevine varieties. Vitis / herausgegeben im Auftrage der Bundesforschungsanstalt für Rebenzuchtung Geilweilerhof **26**, 192–192.

Bondada BR, Syvertsen JP. 2003. Leaf chlorophyll, net gas exchange and chloroplast ultrastructure in citrus leaves of different nitrogen status. Tree physiology **23**, 553–559.

Borruso L, Bani A, Pioli S, Ventura M, Panzacchi P, Antonielli L, Giammarchi F, Polo A, Tonon G, Brusetti L. 2021. Do Aerial Nitrogen Depositions Affect Fungal and Bacterial Communities of Oak Leaves? Frontiers in microbiology **12**, 633535.

Bortolami G, Farolfi E, Badel E, *et al.* 2021*a*. Seasonal and long-term consequences of esca grapevine disease on stem xylem integrity. Journal of experimental botany **72**, 3914–3928.

Bortolami G, Gambetta GA, Cassan C, Dayer S, Farolfi E, Ferrer N, Gibon Y, Jolivet J, Lecomte P, Delmas CEL. 2021*b*. Grapevines under drought do not express esca leaf symptoms. Proceedings of the National Academy of Sciences of the United States of America **118**.

Bortolami G, Gambetta GA, Delzon S, *et al.* 2019. Exploring the hydraulic failure hypothesis of esca leaf symptom formation. Plant physiology **181**, 1163–1174.

Broadhurst D, Goodacre R, Reinke SN, Kuligowski J, Wilson ID, Lewis MR, Dunn WB. 2018. Guidelines and considerations for the use of system suitability and quality control samples in mass spectrometry assays applied in untargeted clinical metabolomic studies. Metabolomics: Official journal of the Metabolomic Society **14**, 72.

Bruez E, Baumgartner K, Bastien S, Travadon R, Guerin-Dubrana L, Rey P. 2016. Various fungal communities colonise the functional wood tissues of old grapevines externally free from grapevine trunk disease symptoms. Australian journal of grape and wine research **22**, 288–295.

Bruez E, Vallance J, Gautier A, Laval V, Compant S, Maurer W, Sessitsch A, Lebrun M-H, Rey P. 2020. Major changes in grapevine wood microbiota are associated with the onset of esca, a devastating trunk disease. Environmental microbiology **22**, 5189–5206.

Bruez E, Vallance J, Gerbore J, Lecomte P, Da Costa J-P, Guerin-Dubrana L, Rey P. 2014. Analyses of the Temporal Dynamics of Fungal Communities Colonizing the Healthy Wood Tissues of Esca Leaf-Symptomatic and Asymptomatic Vines. (BA Vinatzer, Ed.). PloS one **9**, e95928.

Bryant JP, Chapin FS, Klein DR. 1983. Carbon/Nutrient Balance of Boreal Plants in Relation to Vertebrate Herbivory. Oikos **40**, 357–368.

Calzarano F, Amalfitano C, Seghetti L, Cozzolino V. 2009. Nutritional status of vines affected with esca proper. Phytopathologia mediterranea **48**, 20–31.

Claverie M, Audras M, Berud F, Richy D. 2024. Grapevine vigour: a critical factor driving Trunk Disease expression. bioRxiv, 2024.06.11.598450.

Claverie M, Notaro M, Fontaine F, Wery J. 2020. Current knowledge on Grapevine Trunk Diseases with complex etiology: a systemic approach. Phytopathologia mediterranea **59**, 29–53.

Dablanc A, Hennechart S, Perez A, Cabanac G, Guitton Y, Paulhe N, Lyan B, Jamin EL, Giacomoni F, Marti G. 2024. FragHub: A mass spectral library data integration workflow. Analytical chemistry doi: 10.1021/acs.analchem.4c02219.

Danial DL, Parlevliet JE. 1995. Effects of nitrogen fertilization on disease severity and infection type of yellow rust on wheat genotypes varying in quantitative resistance. Journal of phytopathology **143**, 679–681.

Decros G, Baldet P, Beauvoit B, Stevens R, Flandin A, Colombié S, Gibon Y, Pétriacq P. 2019. Get the balance right: ROS homeostasis and redox signalling in fruit. Frontiers in plant science **10**, 1091.

Del Frari G, Gobbi A, Aggerbeck MR, Oliveira H, Hansen LH, Ferreira RB. 2019. Characterization of the wood mycobiome of *Vitis vinifera* in a vineyard affected by esca. Spatial distribution of fungal communities and their putative relation with leaf symptoms. Frontiers in plant science **10**, 910.

Dell'Acqua N, Gambetta GA, Delzon S, Ferrer N, Lamarque LJ, Saurin N, Theodore P, Delmas CEL. 2023. Mechanisms of grapevine resilience to a vascular disease: investigating stem radial growth, xylem development, and physiological acclimation. Annals of botany doi: 10.1093/aob/mcad188.

Destrac-Irvine A, Goutouly J-P, Laveau C, Guérin-Dubrana L. 2007. L'écophysiologie de la vigne. Mieux comprendre les maladies de dépérissement. *L'Union Girondine des Vins de Bordeaux,* **1035**, 28-32.

Destrac A, van Leeuwen C. 2016. VitAdapt: an experimental program to study the behavior of a wide range of Vitis vinifera varieties in a context of climate change in the Bordeaux vineyards. Climwine, sustainable grape and wine production in the context of climate change, 11-13 April 2016, Bordeaux. Full text proceedings paper, 165-171.

Dewasme C, Mary S, Darrieutort G, Roby J-P, Gambetta GA. 2022. Long-term esca monitoring reveals disease impacts on fruit yield and wine quality. Plant disease **106**, 3076–3082.

Dinu DG, Popescu CF, Sumedrea DI, Manolescu AE, Pandelea LM, Rustioni L. 2022. A new strategy to improve vineyard resilience: grapevine morphological adaptation to short-term nitrogen deficiency. Agronomy **12**, 1355.

Djoumbou Feunang Y, Eisner R, Knox C, *et al.* 2016. ClassyFire: automated chemical classification with a comprehensive, computable taxonomy. Journal of cheminformatics **8**, 61.

Dordas C. 2008. Role of nutrients in controlling plant diseases in sustainable agriculture. A review. Agronomy for Sustainable Development **28**, 33–46.

Dussarrat T, Prigent S, Latorre C, *et al.* 2022. Predictive metabolomics of multiple Atacama plant species unveils a core set of generic metabolites for extreme climate resilience. The New phytologist **234**, 1614–1628.

Elena G, Bruez E, Rey P, Luque J. 2018. Microbiota of grapevine woody tissues with or without esca-foliar symptoms in northeast Spain. Phytopathologia mediterranea **57**, 425–438.

Escudié F, Auer L, Bernard M, Mariadassou M, Cauquil L, Vidal K, Maman S, Hernandez-Raquet G, Combes S, Pascal G. 2018. FROGS: Find, Rapidly, OTUs with Galaxy Solution. Bioinformatics **34**, 1287–1294.

Etienne L, Fabre F, Martinetti D, Frank E, Michel L, Bonnardot V, Guérin-Dubrana L, Delmas CEL. 2024. Exploring the role of cultivar, year and plot age in the incidence of esca and Eutypa dieback: Insights from 20 years of regional surveys in France. Plant pathology doi: 10.1111/ppa.13975.

Evans JR. 1989. Photosynthesis and nitrogen relationships in leaves of C3 plants. Oecologia **78**, 9–19.

Fagard M, Launay A, Clément G, Courtial J, Dellagi A, Farjad M, Krapp A, Soulié M-C, Masclaux-Daubresse C. 2014. Nitrogen metabolism meets phytopathology. Journal of experimental botany **65**, 5643–5656.

Fan H, Quan S, Ye Q, *et al.* 2023. A molecular framework underlying low-nitrogen-induced early leaf senescence in Arabidopsis thaliana. Molecular plant **16**, 756–774.

Ferrario-Méry S, Thibaud M-C, Betsche T, Valadier M-H, Foyer CH. 1997. Modulation of carbon and nitrogen metabolism, and of nitrate reductase, in untransformed and transformed *Nicotiana plumbaginifolia* during CO 2 enrichment of plants grown in pots and in hydroponic culture. Planta **202**, 510–521.

Fortier E, Desjardins Y, Tremblay N, Bélec C, Côté M. 2010. Influence of irrigation and nitrogen fertilization on broccoli polyphenolics concentration. Acta horticulturae **856**, 55–62.

Fritz C, Palacios-Rojas N, Feil R, Stitt M. 2006. Regulation of secondary metabolism by the carbon-nitrogen status in tobacco: nitrate inhibits large sectors of phenylpropanoid metabolism. The Plant journal: for cell and molecular biology **46**, 533–548.

Gastou P, Destrac Irvine A, Arcens C, Courchinoux E, This P, Van Leeuwen C, Delmas C. 2024. Large gradient of susceptibility to esca disease revealed by long-term monitoring of 46 grapevine cultivars in a common garden vineyard. OENO One **58**.

Herms DA, Mattson WJ. 1992. The dilemma of plants: To grow or defend. The Quarterly review of biology **67**, 283–335.

Hernández I, Alegre L, Van Breusegem F, Munné-Bosch S. 2009. How relevant are flavonoids as antioxidants in plants? Trends in plant science **14**, 125–132.

Hoffland E, van Beusichem ML, Jeger MJ. 1999. Nitrogen availability and susceptibility of

tomato leaves to *Botrytis cinerea*. Plant and soil **210**, 263–272.

Hoffland E, Jeger MJ, van Beusichem ML. 2000. Effect of nitrogen supply rate on disease resistance in tomato depends on the pathogen. Plant and soil **218**, 239–247.

Huber DM, Watson RD. 1974. Nitrogen Form and Plant Disease. Annual review of phytopathology **12**, 139–165.

Jackson DI, Lombard PB. 1993. Environmental and Management Practices Affecting Grape Composition and Wine Quality - A Review. American journal of enology and viticulture **44**, 409–430.

Keller M, Arnink KJ, Hrazdina G. 1998. Interaction of nitrogen availability during bloom and light intensity during veraison. I. Effects on grapevine growth, fruit development, and ripening. American journal of enology and viticulture **49**, 333–340.

Keller M, Kummer M, Vasconcelos MC. 2001. Reproductive growth of grapevines in response to nitrogen supply and rootstock. Australian journal of grape and wine research **7**, 12–18.

Keller M, Rogiers S, Schultz H. 2003. Nitrogen and ultraviolet radiation modify grapevines' susceptibility to powdery mildew. Vitis -Geilweilerhof- **42**, 87–94.

Lecomte P, Bénétreau C, Diarra B, Meziani Y, Delmas C, Fermaud M. 2024. Logistic modeling of summer expression of esca symptoms in tolerant and susceptible cultivars in Bordeaux vineyards. OENO One **58**.

Lecomte P, Darrieutort G, Liminana J-M, Comont G, Muruamendiaraz A, Legorburu F-J, Choueiri E, Jreijiri F, El Amil R, Fermaud M. 2012. New insights into esca of grapevine : the development of foliar symptoms and their association with xylem discoloration. Plant disease **96**, 924–934.

Leser C, Treutter D. 2005. Effects of nitrogen supply on growth, contents of phenolic compounds and pathogen (scab) resistance of apple trees. Physiologia plantarum **123**, 49–56.

Liao H-S, Yang C-C, Hsieh M-H. 2022. Nitrogen deficiency- and sucrose-induced anthocyanin biosynthesis is modulated by HISTONE DEACETYLASE15 in Arabidopsis. Journal of experimental botany **73**, 3726–3742.

Lima MRM, Felgueiras ML, Cunha A, Chicau G, Ferreres F, Dias ACP. 2017. Differential phenolic production in leaves of *Vitis vinifera* cv. Alvarinho affected with esca disease. Plant physiology and biochemistry **112**, 45–52.

Lorenz DH, Eichhorn KW, Bleiholder H, Klose R, Meier U, Weber E. 1995. Growth Stages of the Grapevine: Phenological growth stages of the grapevine (Vitis vinifera L. ssp. vinifera)—Codes and descriptions according to the extended BBCH scale. Australian journal of grape and wine research **1**, 100–103.

Luna E, Flandin A, Cassan C, Prigent S, Chevanne C, Kadiri CF, Gibon Y, Pétriacq P. 2020. Metabolomics to Exploit the Primed Immune System of Tomato Fruit. Metabolites **10**.

Lu Y, Zhou G, Ewald J, Pang Z, Shiri T, Xia J. 2023. MicrobiomeAnalyst 2.0:

comprehensive statistical, functional and integrative analysis of microbiome data. Nucleic acids research **51**, W310–W318.

Macheix J-J, Fleuriet A, Jay-Allemand C. 2005. Les composés phénoliques des végétaux: un exemple de métabolites secondaires d'importance économique. PPUR presses polytechniques.

Mallick H, Rahnavard A, McIver LJ, *et al.* 2021. Multivariable association discovery in population-scale meta-omics studies. PLoS computational biology **17**, e1009442.

Marcianò D, Ricciardi V, Maddalena G, Massafra A, Marone Fassolo E, Masiero S, Bianco PA, Failla O, De Lorenzis G, Toffolatti SL. 2023. Influence of nitrogen on grapevine susceptibility to downy mildew. Plants **12**.

Martins J, Pétriacq P, Flandin A, Gómez-Cadenas A, Monteiro P, Pinto G, Canhoto J. 2022. Genotype determines *Arbutus unedo* L. physiological and metabolomic responses to drought and recovery. Frontiers in plant science **13**, 1011542.

Massad TJ, Dyer LA, Vega C G. 2012. Costs of defense and a test of the carbon-nutrient balance and growth-differentiation balance hypotheses for two co-occurring classes of plant defense. PloS one **7**, e47554.

Ma D, Sun D, Wang C, Li Y, Guo T. 2014. Expression of flavonoid biosynthesis genes and accumulation of flavonoid in wheat leaves in response to drought stress. Plant physiology and biochemistry: PPB / Societe francaise de physiologie vegetale **80**, 60–66.

McElrone AJ, Manuck CM, Brodersen CR, Patakas A, Pearsall KR, Williams LE. 2021. Functional hydraulic sectoring in grapevines as evidenced by sap flow, dye infusion, leaf removal and micro-computed tomography. AoB plants **13**, lab003.

McMurdie PJ, Holmes S. 2013. phyloseq: an R package for reproducible interactive analysis and graphics of microbiome census data. PloS one **8**, e61217.

Metay A, Magnier J, Guilpart N, Christophe A. 2015. Nitrogen supply controls vegetative growth, biomass and nitrogen allocation for grapevine (cv. Shiraz) grown in pots. Functional plant biology: FPB **42**, 105–114.

Moret F, Delorme G, Clement G, Grosjean C, Lemaitre-Guillier C, Trouvelot S, Adrian M, Fontaine F. 2020. Esca-affected grapevine leaf metabolome is clone- and vintage-dependent. Physiologia plantarum doi: 10.1111/ppl.13254.

Mugnai L, Graniti A, Surico G. 1999. Esca (black measles) and brown wood-streaking: two old and elusive diseases of grapevines. Plant disease **83**, 404–418.

Mundy DC. 2008. A review of the direct and indirect effects of nitrogen on botrytis bunch rot in wine grapes. New Zealand Plant Protection **61**, 306–310.

Mur LAJ, Simpson C, Kumari A, Gupta AK, Gupta KJ. 2017. Moving nitrogen to the centre of plant defence against pathogens. Annals of botany **119**, 703–709.

Ouadi L, Bruez E, Bastien S, Yacoub A, Coppin C, Guérin-Dubrana L, Fontaine F, Domec J-C, Rey P. 2021. Sap flow disruption in grapevine is the early signal predicting the

structural, functional, and genetic responses to Esca disease. Frontiers in plant science **12**, 695846.

Schreiner R, Lee J, Skinkis PA. 2013. N, P, and K Supply to Pinot noir grapevines: Impact on vine nutrient status, growth, physiology, and yield. American journal of enology and viticulture **64**, 26–38.

Rossouw G, Smith J, Barril C, Deloire A, Holzapfel B. 2017. Implications of the presence of maturing fruit on carbohydrate and nitrogen distribution in grapevines under postveraison water constraints. Journal of the American Society for Horticultural Science. American Society for Horticultural Science **142**, 71–84.

Schoch CL, Seifert KA, Huhndorf S, Robert V, Spouge JL, Levesque CA, Chen W, Fungal Barcoding Consortium, Fungal Barcoding Consortium Author List. 2012. Nuclear ribosomal internal transcribed spacer (ITS) region as a universal DNA barcode marker for Fungi. Proceedings of the National Academy of Sciences of the United States of America **109**, 6241–6246.

Seepaul R, George S, Wright DL. 2016. Comparative response of *Brassica carinata* and *B. napus* vegetative growth, development and photosynthesis to nitrogen nutrition. Industrial crops and products **94**, 872–883.

Snoeijers S, Pérez-García A, Joosten M, De Wit P. 2000. The effect of nitrogen on disease development and gene expression in bacterial and fungal plant pathogens. European journal of plant pathology / European Foundation for Plant Pathology **106**, 493–506.

Soulie M, Koka SM, Floch K, *et al.* 2020. Plant nitrogen supply affects the *Botrytis cinerea* infection process and modulates known and novel virulence factors. Molecular plant pathology **21**, 1436–1450.

Squeri C, Miras-Moreno B, Gatti M, Garavani A, Poni S, Lucini L, Trevisan M. 2021. Gas exchange, vine performance and modulation of secondary metabolism in *Vitis vinifera* L. cv Barbera following long-term nitrogen deficit. Planta **253**, 73.

Stewart AJ, Chapman W, Jenkins GI, Graham I, Martin T, Crozier A. 2001. The effect of nitrogen and phosphorus deficiency on flavonol accumulation in plant tissues. Plant, cell & environment **24**, 1189–1197.

Treutter D. 2006. Significance of flavonoids in plant resistance: a review. Environmental chemistry letters **4**, 147–157.

Tsugawa H, Cajka T, Kind T, Ma Y, Higgins B, Ikeda K, Kanazawa M, VanderGheynst J, Fiehn O, Arita M. 2015. MS-DIAL: data-independent MS/MS deconvolution for comprehensive metabolome analysis. Nature methods **12**, 523–526.

Ullah S, Ai C, Ding W, Jiang R, Zhao S, Zhang J, Zhou W, Hou Y, He P. 2019. The response of soil fungal diversity and community composition to long-term fertilization. Applied soil ecology: a section of Agriculture, Ecosystems & Environment **140**, 35–41.

Van Leeuwen C, Friant P. 2011. Etude de l'impact de trois stratégies au sein des parcelles viticoles dégradées sur le comportement du sol, la physiologie de la vigne et la composition de la baie. Colloque IFV Sud-Ouest - Toulouse.

Verdenal T, Dienes-Nagy Á, Spangenberg JE, Zufferey V, Spring J-L, Viret O, Marin-Carbonne J, van Leeuwen C. 2021. Understanding and managing nitrogen nutrition in grapevine: a review. OENO One **55**, 1–43.

Vitousek P, Howarth R. 1991. Nitrogen limitation on land and in the sea: how can it occur? Biogeochemistry 13:87-115. Biogeochemistry **13**, 87–115.

Vrignon-Brenas S, Aurélie M, Romain L, Shiva G, Alana F, Myriam D, Gaëlle R, Anne P. 2019. Gradual responses of grapevine yield components and carbon status to nitrogen supply: This article is published in cooperation with the 21th GIESCO International Meeting, June 23-28 2019, Thessaloniki, Greece. Guests editors : Stefanos Koundouras and Laurent Torregrosa. OENO One **53**.

Weiller F, Diniz I, Pimentel D, Erban A, Reis P, Soares F, Rego C, Kopka J, Fortes AM. 2024. Metabolomic analysis of grapes and leaves from symptomatic and asymptomatic *Vitis vinifera* grapevines with Esca disease. Current Plant Biology **40**, 100378.

Xie K, Lu Z, Pan Y, Gao L, Hu P, Wang M, Guo S. 2020. Leaf photosynthesis is mediated by the coordination of nitrogen and potassium: The importance of anatomical-determined mesophyll conductance to CO2 and carboxylation capacity. Plant science: an international journal of experimental plant biology **290**, 110267.

Zhang H, Yuan F, Wu J, Jin C, Pivovaroff AL, Tian J, Li W, Guan D, Wang A, McDowell NG. 2021. Responses of functional traits to seven-year nitrogen addition in two tree species: coordination of hydraulics, gas exchange and carbon reserves. (D Tissue, Ed.). Tree physiology **41**, 190–205.

Zhao D, Reddy KR, Kakani VG, Reddy VR. 2005. Nitrogen deficiency effects on plant growth, leaf photosynthesis, and hyperspectral reflectance properties of sorghum. European journal of agronomy: the journal of the European Society for Agronomy **22**, 391–403.

Zheng S, Wang T, Wei X, Li B, Bai Y. 2022. Greenhouse grapevine transpiration and water use efficiency under different water and nitrogen conditions. Irrigation and Drainage Systems **71**, 48–60.

Zinger L, Lionnet C, Benoiston A-S, Donald J, Mercier C, Boyer F. 2021. metabaR: An r package for the evaluation and improvement of DNA metabarcoding data quality. Methods in ecology and evolution / British Ecological Society **12**, 586–592.